

Effects of CO₂ on the Micron-Scale Pore-Fracture Structure and Connectivity in Coals from the Qinshui Basin

Shiqi Liu*, Shuxun Sang, Tian Wang, Yi Du, and Huihuang Fang, China
University of Mining and Technology, Xuzhou, China

Abstract

Changes in the micron-scale pore and fracture structure in coal caused by CO₂ are critical for CO₂ injection and CH₄ production in coal seams. To investigate the effects of CO₂ on the characteristics and connectivity of micrometer-scale pores and fractures in coal, four coal samples from the Qinshui basin were selected. These samples were exposed to CO₂ and water for 240 hours at 80 °C and 20 MPa using a CO₂ geochemical reactor. X-ray micro-CT (computed tomography), field emission scanning electron microscopy (FESEM), and energy dispersive spectroscopy (EDS) were used to identify the characteristics and connectivity of micron-scale pores and fractures in the coal samples before and after CO₂ treatment. Then, the influence of mineral dissolution on micrometer-scale pores and fractures was discussed. After CO₂ treatment, the massive dissolution of carbonate minerals significantly increased the pore contents and volumes of the coal samples. For this reason, the grain size and volume of carbonate minerals determined the increase in pore number and volume after CO₂ treatment. The dissolution of calcite, dolomite, and other carbonate minerals in the coal matrix formed a large number of pores created by dissolution <10 μm in diameter, which affected the number of pores in the coal after CO₂ treatment, but contributed little to the connectivity of the coal at the micro-scale. The carbonate minerals that filled the microfractures were heavily dissolved in CO₂, increasing the aperture and connectivity of the microfractures. The dissolution of carbonate minerals in microfractures was the major contributor to the increase in the volume of pores >50 μm in diameter and the main reason for the increase in coal connectivity at the micrometer scale.

Introduction

The adsorption of CO₂ is superior to that of CH₄ in coal seams (Day et al. 2008; White et al. 2005). By injecting and storing CO₂ in coal seams, CH₄ can be displaced by CO₂ and expelled from the coal seam, thereby improving CH₄ recovery and reducing CO₂ emissions (White et al. 2005; Hol et al. 2014; Fujioka et al. 2010). This technique is called CO₂ geological storage-enhanced coalbed methane recovery (CO₂-ECBM). CO₂-ECBM has environmental and energy benefits and has quickly become one of the hot spots in research on coalbed methane and emissions reduction (Hol et al. 2014; Fujioka et al. 2010). The United States, Canada, the Netherlands, Japan, and China have conducted pilot tests of CO₂-ECBM, and the results are satisfactory (Fujioka et al. 2010; Faiz et al. 2007; Pan et al. 2018; Wong et al. 2007).

Mixing of CO₂ and water forms an acid fluid containing H₂CO₃, which can dissolve calcite, dolomite, magnesite, and other minerals and promote Ca and Mg migration (Bertier et al. 2006; Dawson et al. 2015; Du et al. 2018; Hayashi et al. 1991; Kolak and Burruss 2014; Liu et al. 2018). The CO₂-induced migration, dissolution and precipitation of inorganic minerals in coal change the structure of the coal, eg, opening some closed and semi-closed pores in the coal, changing the distribution of pore size in the coal, and increasing the porosity and permeability of the coal (Anggara et al. 2013; Kutchko et al. 2013; Liu et

al. 2015; Liu et al. 2010 ;Massarotto et al. 2010; Liu et al. 2019). CO₂ can also dissolve minerals filling coal fractures, thus increasing the aperture and connectivity of coal fractures and changing the mechanical properties of the coal (Anggara et al. 2013; Massarotto et al. 2010; Perera et al. 2011; Ranjith and Perera 2012). Other scholars have suggested that the reaction between the CO₂-H₂O system and coal is a long-term process in which dissolved mineral components can migrate and precipitate in fractures that have not been filled with minerals or dissolved with CO₂, thus reducing their connectivity (Du et al. 2018; Kutchko et al. 2013; Xu et al. 2016; Zerai et al. 2006).

The characteristics and connectivity of pores and fractures in coal determine the storage, diffusion, and migration of CH₄ and CO₂ in coal (Liu et al. 2015; Wang et al. 2017; Zhou et al. 2018). It is generally believed that the micron-scale pores in coal are mainly secondary gas pores and dissolution-created pores, while the fractures are micro-fractures and some small-scale cleats (Liu et al. 2015; Liu et al. 2016; Liu et al. 2017). These pores and fractures are the main seepage channels of CH₄ and CO₂ and connect the microscopic structure (e.g., adsorption pores and diffusion pores) and the macroscopic structure (e.g., macroscopic fractures) of the coals (Liu et al. 2015; Liu et al. 2016; Liu et al. 2017). Therefore, changes in the characteristics and connectivity of micron-scale pores and fractures in coal determine the injectivity and storage capacity of CO₂ and the production of CH₄, which are crucial factors in CO₂-ECBM. Research on changes in coal structures caused by CO₂ reactions was mainly focused on the nano- to sub-micrometer scale and the macroscale. The changes in the characteristics and connectivity of pores and fractures at the micron-scale are still unclear.

In this paper, using typical low-volatile bituminous coal and anthracite coal as examples, X-ray microCT (computed tomography), field emission scanning electron microscopy (FESEM), and energy disperse spectroscopy (EDS) were used to study the effects and mechanisms of CO₂ on the characteristics and connectivity of micrometer-scale pores and fractures in coal. This study aims to provide a better understanding of the effectiveness of CO₂ injection and CH₄ production.

Samples and Methodology

Samples. Four groups of coal samples were collected from the Qinshui basin, China, including low-volatile bituminous coal from the Xinyuan Mine, semi-anthracite coal from the Yuwu Mine and the Xinjing Mine, and anthracite coal from the Sihe Mine. These samples were named Coal #1 to Coal #4 (Table 1). The coal samples were systematically collected from the working faces of the coal mines. The collection, retention, and preparation of the coal samples were conducted in line with the relevant standard GB/T 19222-2003 in China and the international standard ISO 7404-2:1985. To prevent further oxidization, coal samples were wrapped in absorbent paper, hermetically sealed in plastic bags and stored at 5 °C after sample collection. The key properties of these samples are shown in Table 1.

Table 1—Properties of the coals used.

Samples	Sampling location	$R_{o, \max}$ (%)	Proximate (wt. %)				Ultimate (wt. %)			
			M_{ad}	A_{ad}	V_{daf}	FC_{ad}	O_{daf}	C_{daf}	H_{daf}	N_{daf}
#1	Xinyuan Mine	1.81	0.81	5.35	15.26	80.20	9.30	80.32	4.43	1.14
#2	Yuwu Mine	2.19	1.10	11.98	13.44	76.19	2.44	91.73	4.12	2.44
#3	Xinjing Mine	2.64	1.66	10.02	10.10	80.89	3.05	91.52	3.96	1.06
#4	Sihe Mine	3.33	1.48	13.12	6.32	81.39	2.98	93.45	2.15	1.00

Note: $R_{o, \max}$, the mean maximum reflectance values of vitrinite; wt. %, weight percent; M_{ad} , moisture; A_{ad} , ash yield; V_{daf} , volatile matter; FC_{ad} , fixed carbon content; O_{daf} , oxygen content; C_{ad} , carbon content; H_{ad} , hydrogen content; N_{daf} , nitrogen content; “ad” means air-dried basis; “daf” means dry ash-free basis.

CO₂ Treatment. CO₂ treatments were performed to replicate a burial depth of 2000 m. The temperature and pressure at this burial depth (80 °C and 20 MPa, respectively) were calculated from the temperature and depth of the sub-surface constant temperature zone, the average geothermal gradient, and the average pressure gradient at the sampling location. The coal samples chosen for CO₂ treatment consisted of small coal pillars for X-ray CT and bulk coal for scanning electron microscopy (SEM) analysis. Details of the high-pressure reactor and the experimental duration used in CO₂ treatment can be found in our previous

studies (Liu et al. 2018; Liu et al. 2019). After the CO₂ treatment, the coal samples were vacuum dried at 50 °C for 24 hours for the X-ray CT scan and SEM analysis.

Pore-fracture Network Modelling. X-ray CT scan. X-ray CT scanning was performed with an Xradia 520 Versa X-ray CT scanner produced by the Carl Zeiss Foundation Group. Samples for X-ray CT scanning were small coal pillars approximately 2 mm in diameter and 2 mm in height. These were drilled from bulk coal samples using a mechanical sampler.

The scanning area of the X-ray CT scan was 1 mm in diameter and 1 mm in height. The total scan number was 1000 and the voxel resolution was 1.0 μm. After the X-ray CT scan, the small coal pillars were loaded into 800 mesh nylon bags that are resistant to high temperatures and corrosion for CO₂ treatment. After CO₂ treatment, X-ray CT scans were taken again of the small coal pillars. To compare the X-ray CT results, the scanning range, total scan number, voxel resolution, and scanning position of the small coal pillars before and after CO₂ treatment were the same. To ensure the same scanning areas before and after CO₂ treatment, the central point of each small coal pillar was identified as the center of the scanning area. Due to the manually set scanning area, slight errors may exist. However, the X-ray CT results show that these errors have a weak impact on the research and can be ignored.

Establishing the pore-fracture network model. Three-dimensional (3D) digital models of coal were established using Avizo 9, which is professional software for 3D digital cores based on X-ray CT images. The process of establishing the 3D digital model of the coal includes several steps, such as 3D imaging reconstruction, image denoising, image binarization, and model construction. Threshold selection is the key to identifying pores and fractures during the binarization process. In this paper, the X-ray CT images were first converted into 8-bit TIFF bitmaps (Tag image file format), and then their greyscales were normalized to the range of 0-255. Thus, all bitmaps had 256 greyscales and the same grey range. Threshold segmentation of the X-ray CT images revealed that the grey ranges for pore fractures, organic matter and minerals are 0-110, 110-180 and 180-255, respectively.

Based on the 3D digital model of coal, the characteristics of pores, fractures and minerals, including porosity, pore size distribution, pore volumes, mineral grain size distribution, and mineral volumes, were further extracted. The maximum inscribed ball method was used to extract the pore size and grain size of the mineral, and the equivalent diameters (EqDiameters) of the pores and minerals were obtained. Furthermore, the equivalent pore-fracture network models which are ball-and-stick models, and interconnected pore-fracture models, were established, and the coordination numbers of pores and fractures and throat lengths were extracted. Due to the large number of calculations and limited calculation capacity of the workstation, cubic ball-and-stick models and interconnected pore-fracture network models of coal samples that were 500 μm on each side were established.

According to the maximum inscribed ball method, the fractures are filled with a number of balls and cut into a number of pores. Therefore, the contents, volumes, and numbers of pores extracted from the 3D digital model contain the contents, volumes, and numbers of fractures. When establishing the ball-and-stick model, a series of balls filling the fractures are identified as throats. For this reason, fractures are generally considered throats in the ball-and-stick model.

Scanning Electron Microscopy Analysis. Pores, micro-fractures, and minerals in coal before and after CO₂ treatment were investigated using a Sigma 300 FESEM instrument produced by the Carl Zeiss Foundation Group, Germany, with a QUANTAX 200 EDS produced by Bruker Company, USA, with amplification from 10³ to 10⁵. Samples used for FESEM were bulk coal. The coal samples were polished into small samples approximately 10-30 mm across and 4-5 mm high using a polishing and burnishing machine. Then, the small samples of coal were polished using a cross section polisher. After FESEM analysis, coal samples were first loaded into 800 mesh nylon bags for CO₂ treatment and then investigated again using FESEM to observe changes in pores, fracture, and minerals after CO₂ treatment.

Coal is known as a non-conducting substance. Therefore, to achieve better experimental results, a thin gold coating is commonly applied to coal samples by sputtering. In this study, the gold coating can hamper reactions between coal samples and CO₂. Therefore, instead of a gold coating, before CO₂ treatment, the sub-face and side faces of each coal sample were wrapped in conductive tape. After CO₂ treatment, to achieve better experimental results, a thin gold coating was applied to the coal samples by sputtering. The grain size of the mineral is small in coal and the minerals are difficult to locate. A

photograph of the minerals was first taken using the back-scattering mode with low amplification. With the help of the Advanced Mineral Identification and Characterization System (AMICS), the mineral compositions were initially identified, and the typical minerals were marked in the photographs. Then, using the secondary electron mode and increasing the amplification step by step, details on the surface of typical minerals were observed. AMICS is the latest software package for automated identification and quantification of minerals and synthetic phases (Du et al. 2018). Combined with EDS, AMICS can be used to synthesize SEM images and automatically determine the compositions of minerals with grain sizes greater than 4 μm via an amplification of 200 (Du et al. 2018).

Results and Discussion

Changes in Pore Structure. Pore Content. Before CO_2 treatment, the pore contents of the coal samples are relatively low, ranging from 0.84-2.18 % (Table 2). After CO_2 treatment, the pore contents (1.22-5.93 %) of the coal samples increase significantly, with an average increase of 82.61 % (Table 2). Changes in pore volumes show the same trend as changes in pore contents (Table 2).

Table 2—Volumes and contents of pores and minerals in coal samples based on X-ray CT.

Samples	Pore content, %		Mineral content, %		Pore volume, μm^3		Mineral volume, μm^3	
	Before	After	Before	After	Before	After	Before	After
#1	2.18	3.33	5.43	3.33	1.62E+07	2.46E+07	4.01E+07	2.46E+07
#2	1.20	1.54	3.77	2.83	8.86E+06	1.14E+07	2.78E+07	2.09E+07
#3	1.95	5.93	8.18	3.73	1.48E+07	4.50E+07	6.22E+07	2.83E+07
#4	0.84	1.22	3.19	2.40	2.03E+07	2.98E+07	7.72E+07	5.86E+07

Pore Number. Before CO_2 treatment, the pores in the coal samples are primarily $<5 \mu\text{m}$ in eqDiameter, and the pore number decreases rapidly with increasing pore eqDiameter (Figure 1). The number of pores $>10 \mu\text{m}$ in eqDiameter is small (Figure 1). After CO_2 treatment, the number of pores $<2 \mu\text{m}$ of Coal Sample #2 changes slightly, while the number in the other coal samples decreases (Figure 1). The number of pores ranging from 2-10 μm in eqDiameter of Coal Sample #3 decreases, while the number of the other coal samples increases slightly (Figure 1). Moreover, the number of pores $>10 \mu\text{m}$ in eqDiameter changes slightly (Figure 1). In general, changes in pore number are not significant, indicating that changes in pore content and volume are not determined by changes in pore number.

Pore Volume. Before CO_2 treatment, the pore volumes of the coal samples are primarily associated with pores $<10 \mu\text{m}$ in eqDiameter, with pores $>10 \mu\text{m}$ in eqDiameter accounting for a small volume (Figure 2). The volumes of pores $<50 \mu\text{m}$ in eqDiameter follow normal distribution, and the peak of pore volume ranges from 3 to 4 μm (Figure 2). With the increase and decrease in the pore eqDiameter, the pore volumes of the coal samples decrease rapidly (Figure 2). Coal Sample #3 and #4 have larger pores $>50 \mu\text{m}$ in eqDiameter, which may result from the presence of micro-fractures (Figure 2). Combined with the pore number distribution, pores $>10 \mu\text{m}$ in eqDiameter contribute greatly to the pore volume. After CO_2 treatment, the pore volume distribution of the coal samples changes significantly, which is mainly caused by the significant increase in the volumes of pores $>50 \mu\text{m}$ in eqDiameter (Figure 2). In addition, the volumes of pores $<50 \mu\text{m}$ in eqDiameter of Coal Sample #2 exhibit no marked changes, while the volumes of pores $<4 \mu\text{m}$ in eqDiameter in Coal Sample #1, #3, and #4 decrease slightly (Figure 2).

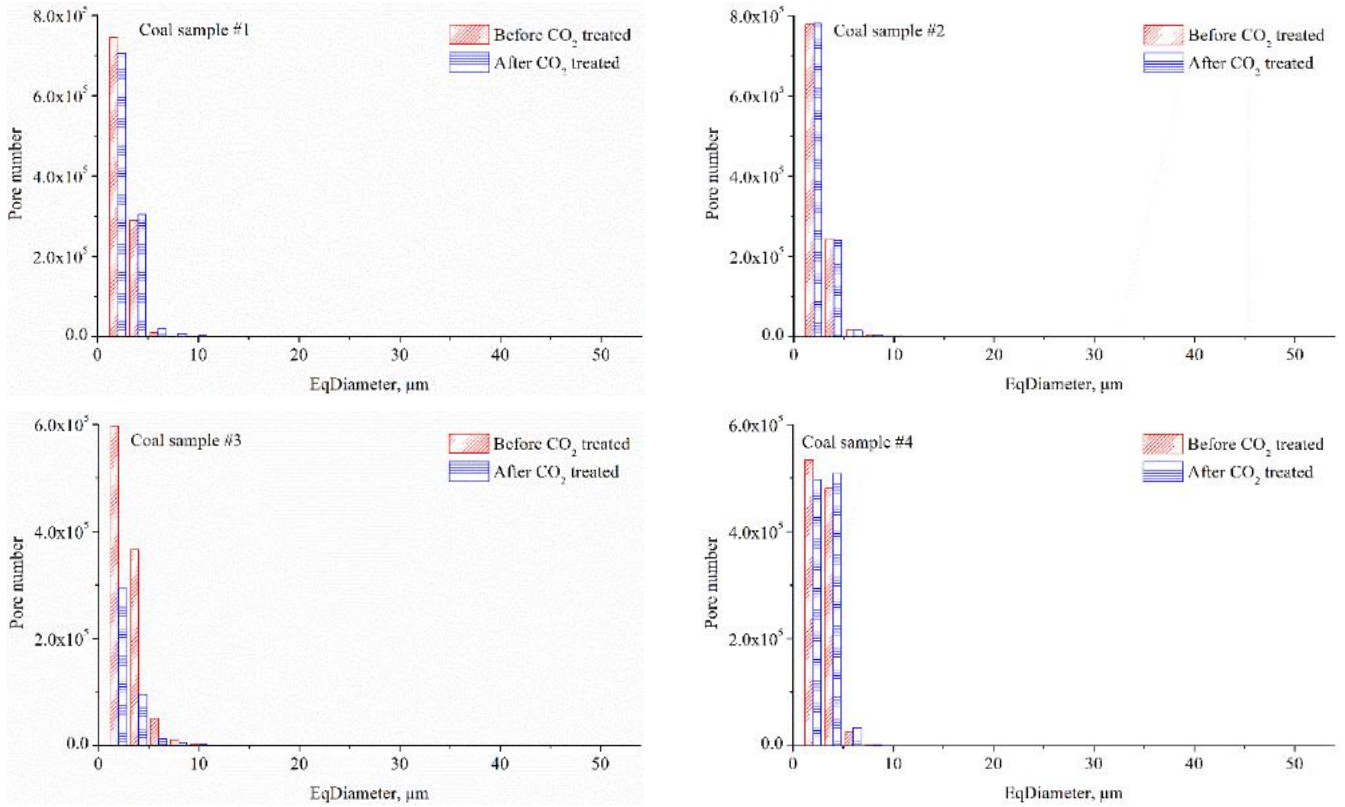


Figure 1—Pore number distribution of coal samples based on X-ray CT.

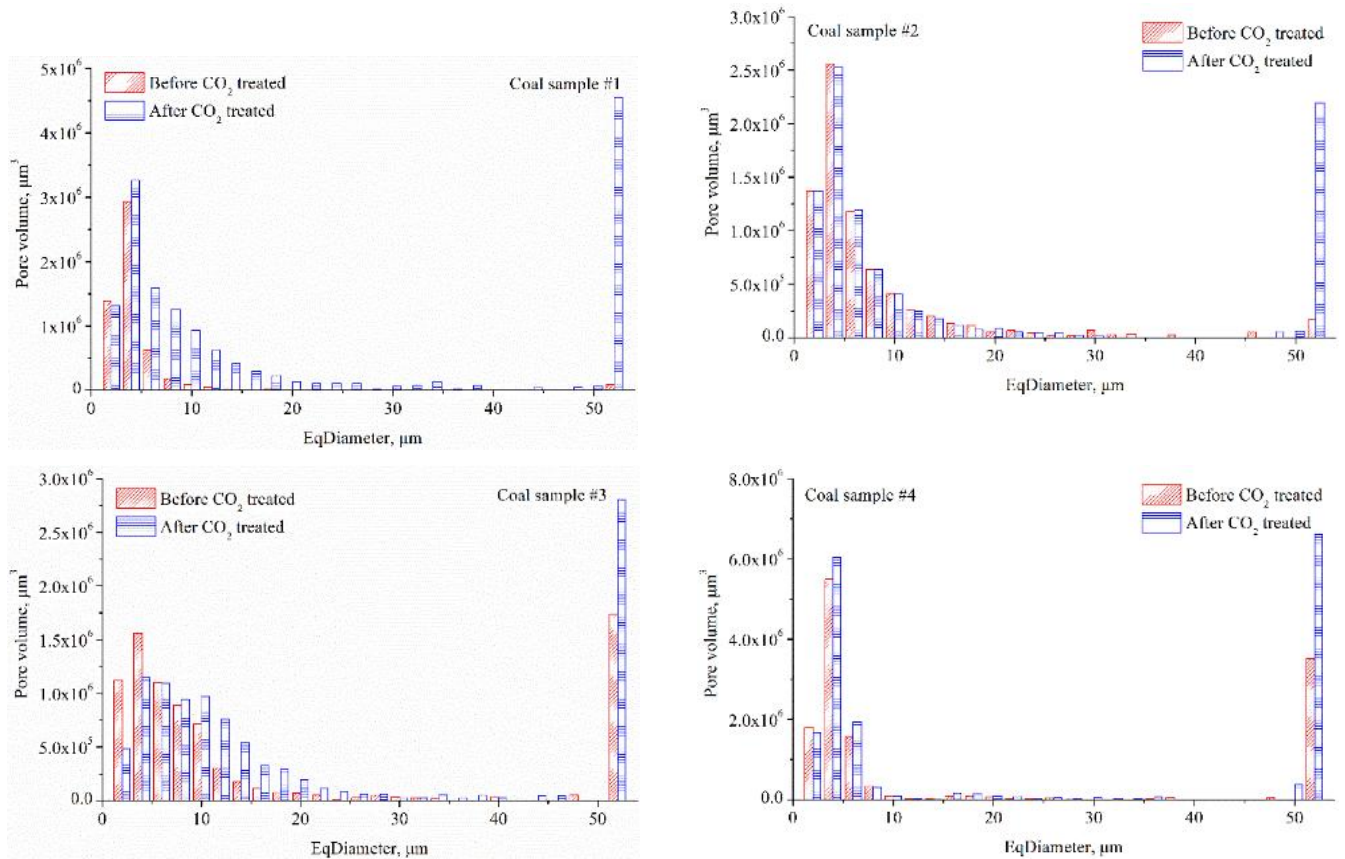
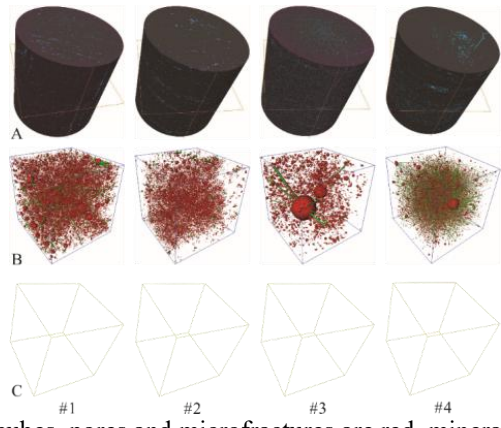


Figure 2—Pore volume distributions of coal samples based on X-ray CT.

Changes in Connectivity. Interconnected Pore Models of Coal Samples. Before CO₂ treatment, there are a large number of pores and a certain number of micro-fractures in the 3D digital models of the coal samples (Figure 3A). The 3D digital models and the ball-and-stick models show that micro-fractures are throats in the ball-and-stick models (Figure 3B). Although some pores and microfractures are connected

(Figure 3B), the connectivity is weak, resulting in poor connectivity in the coal samples. Therefore, the interconnected pore models of the coal samples cannot be extracted (Figure 3C).



Notes: A, 3D digital models of coal; in cubes, pores and microfractures are red, minerals are blue, and organic matter is grey; B, ball-and-stick models of pores and throats; in ball-and-stick models, the pores are red, and the throats are green; and C, interconnected pore models.

Figure 3—3D digital models, ball-and-stick models, and interconnected pore models of coal samples based on X-ray CT before CO₂ treatment.

After CO₂ treatment, some minerals filled the pores and microfractures, increasing the connectivity of the pores and microfractures (Figure 4A). Ball-and-stick models show that the number of pores and throats interconnected in the coal samples increases (Figure 4B). However, the increase in connectivity of pores and micro-fractures caused by CO₂ does not obviously improve the connectivity of the coal samples on the macro-scale (Figure 4C), and the connectivity of pores and micro-fractures is still limited to local areas in the coal samples and does not extend throughout the whole coal samples (Figure 4C). After CO₂ treatment, the interconnected pore models of Coal Sample #1 and Coal Sample #2 were successfully extracted (Figure 4C). By comparing the interconnected pore models and 3D digital models of Coal Samples #1 and #2, the connectivity of coal samples is improved by a micro-fracture (Figure 4A and 4C), which means that the connectivity of coal samples on the micron-scale is mainly contributed by micro-fractures, while the contribution of pores is weak.

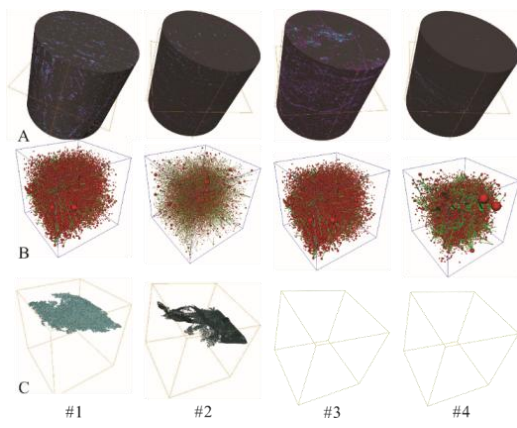


Figure 4—3D digital models, ball-and-stick models, and interconnected pore models of coal samples based on X-ray CT after CO₂ treatment.

Coordination Numbers. The coal samples are dominated by isolated pores (pores with a coordination number of 0), and the number of pores with coordination numbers > 0 only accounts for 0.56-7.83 % (Table 3). The coordination numbers of the interconnected pores (pores with coordination numbers >0) are low, mainly 1-2 (Figure 5). The number of pores with a coordination number >2 decreases rapidly

(Figure 5), indicating that the connectivity of pores and fractures on the macro-scale is weak and that pores are only connected with 1-2 adjacent pores and throats.

Table 3—Numbers and contents of pores with different coordination numbers.

Samples	Pore number						Pore content, %			
	Before			After			Before		After	
	0	>0	Total	0	>0	Total	0	>0	0	>0
#1	1029934	16289	1046223	1005892	34226	1040118	98.44	1.56	96.71	3.29
#2	961181	81686	1042867	948262	94502	1042764	92.17	7.83	90.94	9.06
#3	1021998	5804	1027802	343714	69641	413355	99.44	0.56	83.15	16.85
#4	982578	60727	1043305	968959	73782	1042741	94.18	5.82	92.92	7.08

Notes: “0”, pores with a coordination number of 0; ”>0”, pores with coordination numbers >0.

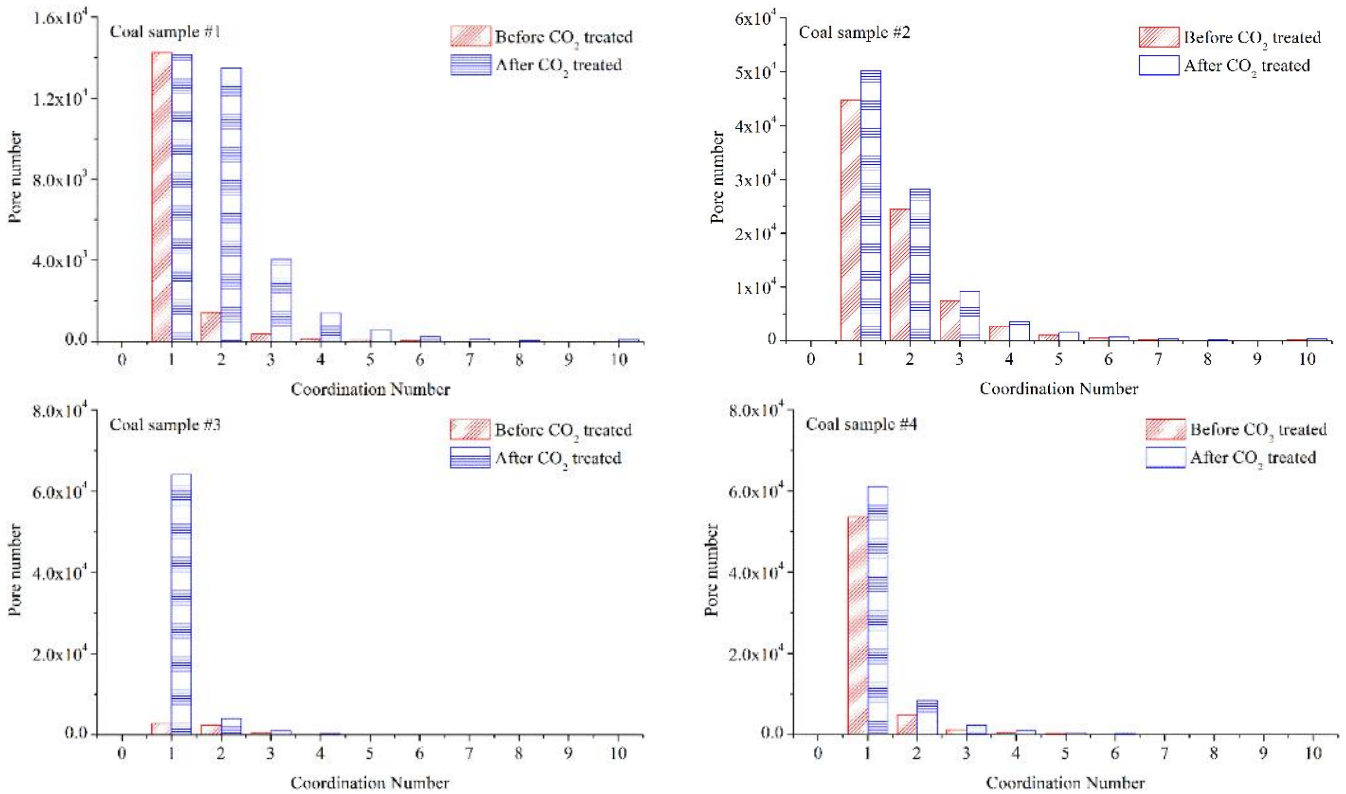


Figure 5—Coordination numbers of coal samples based on X-ray CT.

After CO₂ treatment, the total number of pores in coal samples remained unchanged, except for Coal Sample #3 (Table 3). The number of pores with coordination numbers >0 increases, while the number of pores with a coordination number of 0 decreases correspondingly (Table 3), indicating that CO₂ improves the connectivity of the pores in coal and has little influence on the number of pores. Although the total number of pores and the number of pores with a coordination number of 0 in Coal Sample #3 decrease, the number of pores with coordination numbers >0 increases significantly (Table 3). This is because a large number of pores in Coal Sample #3 become connected to form larger pores. The number of pores with coordination numbers >1 in coal samples all increases (Figure 5), indicating that CO₂ improves the connectivity of pores and fractures in coal to a certain extent.

Throat Lengths. A throat is the connecting channel between pores and is representative of the connectivity of pores and fractures (Song et al. 2018). Before CO₂ treatment, throats <20 μm in length and >100 μm in length are the most common (Figure 6). Throats >100 μm in length are mainly composed of microfractures.

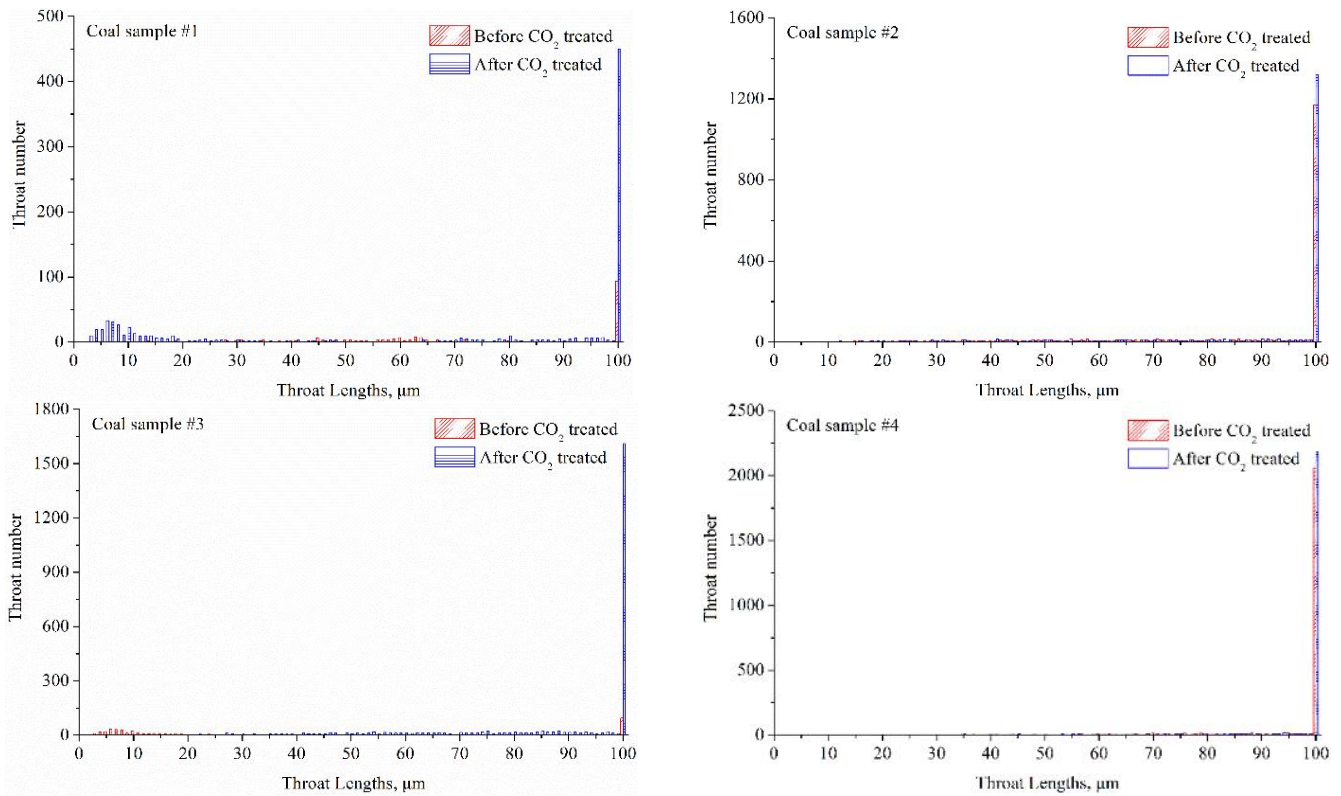


Figure 6—Throat lengths of coal samples based on X-ray CT.

After CO₂ treatment, the number of throats >100 μm in length obviously increases (Figure 6). The number of throats <100 μm in length in Coal Samples #2 and #4 changes weakly (Figure 6). The number of throats <20 μm in length in Coal Sample #1 increases obviously, while the number in Coal Sample #3 decreases (Figure 6). The number of 20-100 μm long throats in Coal Sample #1 does not show obvious changes, while the number in Coal Sample #3 obviously increases (Figure 6).

Changes in Mineral. Similarly to the distribution of the pores, the mineral grain size is mainly <5 μm, and as the grain size increases, the mineral number decreases rapidly (Figure 7). Minerals with a grain size <50 μm are normally distributed, and the peaks of mineral volume are distributed at 3-6 μm (Figure 8). With the increase and decrease in the grain size, the mineral volumes of coal samples decrease rapidly (Figure 8). The volumes of minerals with grain sizes ranging from 10-50 μm are small, while those with grain sizes >50 μm are large (Figure 8), indicating that there is a large amount of minerals with grain sizes >50 μm or a large amount of minerals filling the micro-fractures.

After CO₂ treatment, mineral numbers show a significant decrease trend, while the number of minerals with grain sizes <6 μm in Coal Samples #1, #3 and #4 increases significantly, indicating that minerals with grain sizes >6 μm are partially dissolved, resulting in a decrease in grain size (Figure 7). After CO₂ treatment, the volume of minerals with grain sizes >50 μm largely decreases greatly (Figure 8). Moreover, the 3D digital models of the coal samples (Figure 5A, Figure 4A) show that the minerals that fill the micro-fractures are largely dissolved by CO₂, which improves the connectivity of the micro-fractures and increases the pore volume in the coal samples. Therefore, the dissolution of minerals with grain sizes >50 μm and filling microfractures is the main contributor to the decrease in mineral volume in the coal samples and the increase in the volume of pores >50 μm. Some minerals with grain sizes <50 μm are not completely dissolved, resulting in a significant decrease in the volume of minerals with grain sizes of 6-50 μm and a slight increase in the volume of minerals with grain sizes <6 μm in some coal samples (Figure 8).

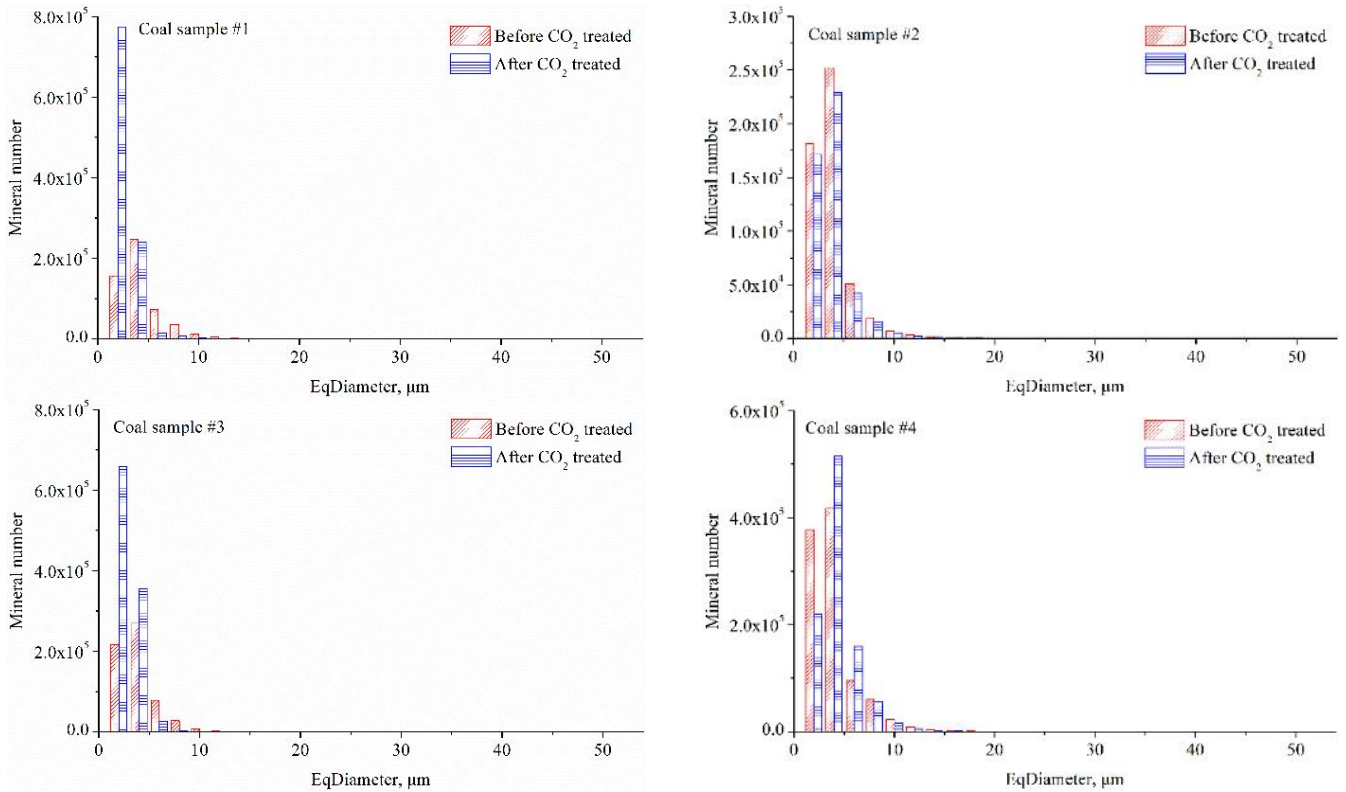


Figure 7—Mineral number distributions in the coal samples based on X-ray CT.

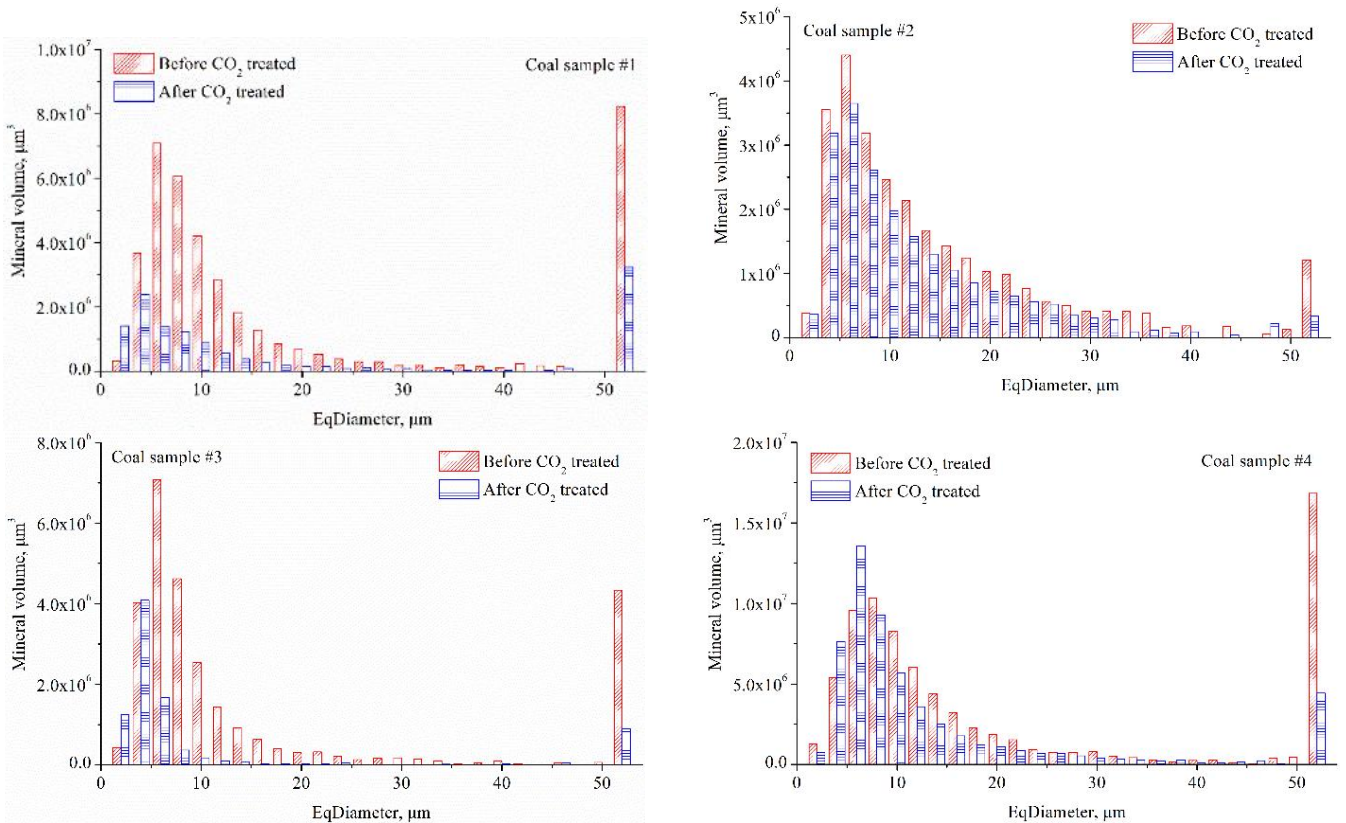


Figure 8—Mineral volume distributions of coal samples based on X-ray CT.

Effects of Mineral Dissolution on Pore Structure. *The Relationship Between Pore Content and Mineral Dissolution.* The mineral contents of the coal samples range from 3.19 % to 8.18 %, and these values decrease significantly (2.40-3.73 %) after CO₂ treatment, with an average decrease of 35.69 % (Table 2). After CO₂ treatment, there are significant positive correlations between increased pore content and decreased mineral content and between pore volume and mineral volume, with $R^2=0.8851$ and

$R^2=0.9624$, respectively (**Figure 9**). These relationships show that the change in the pore content of the coal samples is closely related to the mineral dissolution caused by CO_2 .

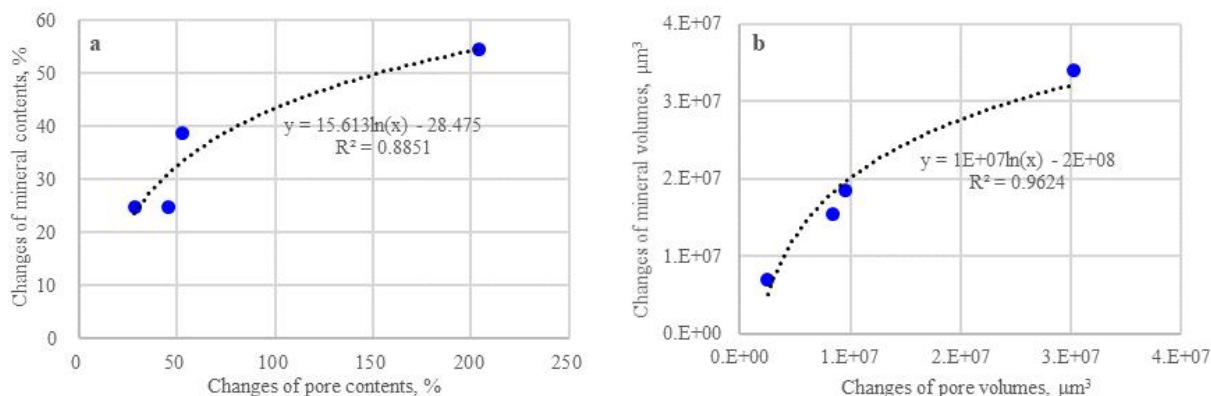


Figure 9—Relationships between pores and minerals before and after CO_2 treatment.

The Effect of Mineral Dissolution on Pore Structure. The minerals with grain sizes $>1 \mu\text{m}$ in the coal samples are mainly clay minerals and carbonate minerals. Clay minerals are mainly kaolinite (46.01 %) and muscovite (13.52 %), and carbonate minerals include calcite (15.98 %), ankerite (1.60%), and dolomite (0.15 %). In addition, there is a certain amount of gibbsite (2.48 %) and organic-clay complex (mainly organic-kaolinite complex) (5.28 %) (Figure 10, Table 4). Clay minerals are mainly distributed in the coal matrix, and minerals filling the microfractures and pores are mainly carbonate minerals and gibbsite, as well as some organic-clay complexes (**Figure 10**).

Table 4—Area percentages of minerals in Coal Sample #2 before and after CO_2 treatment.

Minerals		Kaolinite	Calcite	Muscovite	Ankerite	Gibbsite	Dolomite	Organic-clay complexes	Other minerals
Area percentage, %	Before	46.01	15.98	13.52	1.60	2.48	0.15	5.28	14.98
	After	69.17	0.20	6.14	0.62	3.50	0.20	4.54	15.63

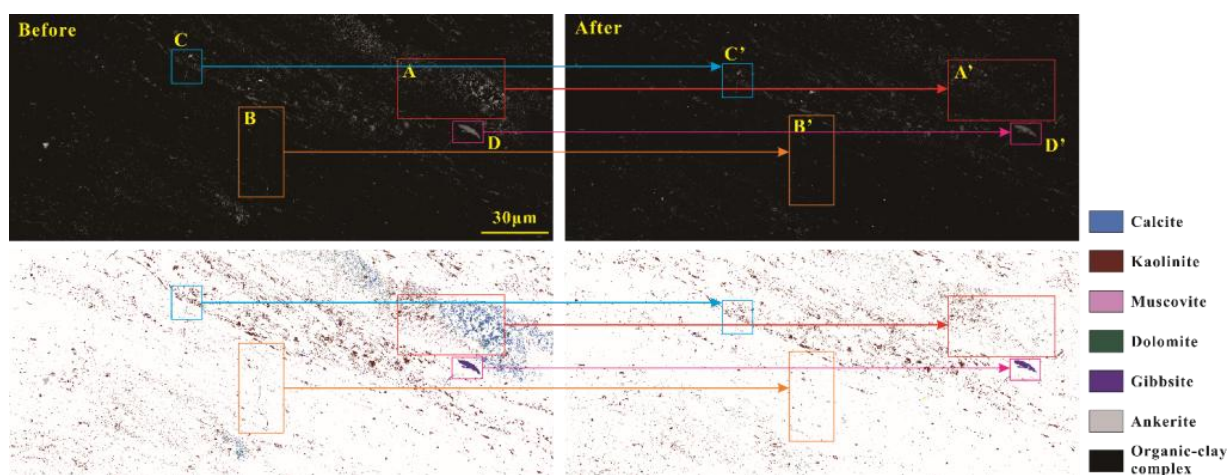
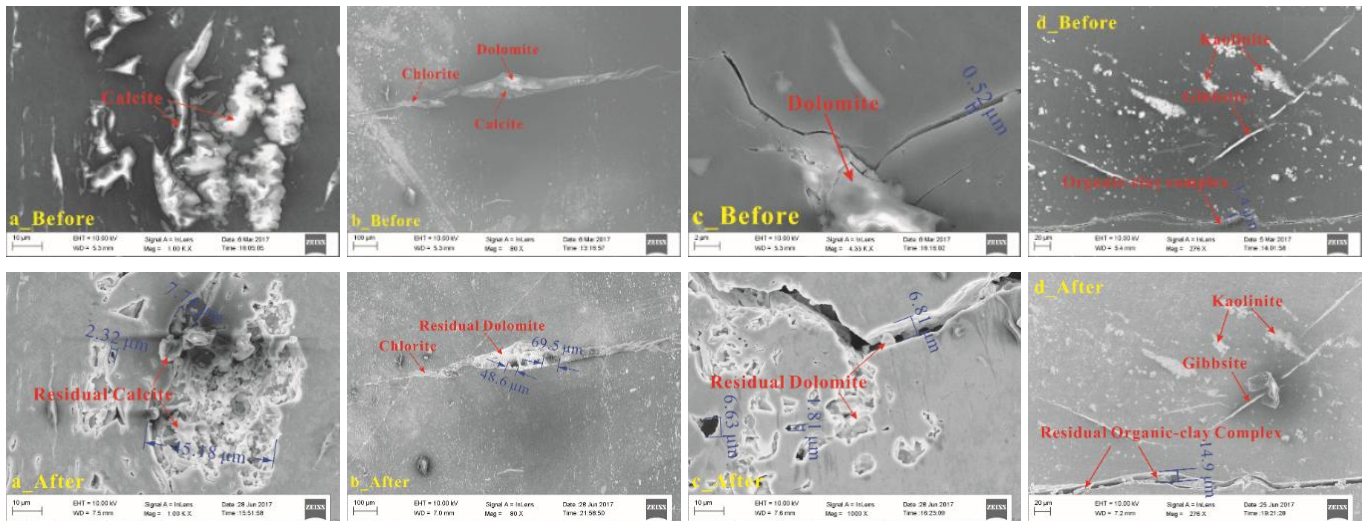


Figure 10—The FESEM and EDS images of Coal Sample #2 before and after CO_2 treatment.

After CO_2 treatment, carbonate minerals are largely dissolved and disappear (Figure 10 AA', BB'). Among them, calcite has the highest degree of dissolution and disappears almost completely (0.20%) (Table 4, Figure 10 AA'), followed by microfractures filled with ankerite (0.62%) (Table 4, Figure 10 BB'). The dolomite in the coal matrix has a relatively low degree of dissolution (0.20 %) (Table 4, Figure 10 AA'), while the dolomite filling micro-fractures is largely dissolved (Figure 10 CC'). Therefore, the dissolution of carbonate minerals is the main reason for the decrease in the mineral content in the coal. Kaolinite reacts weakly with CO_2 . Therefore, kaolinite shows no significant change after CO_2 treatment

(69.17 %) (Table 4, Figure 10 AA'). The gibbsite in the coal matrix is difficult to dissolve with CO₂ (Figure 10 DD'), while the gibbsite filling the micro-fractures is partially dissolved (Figure 10 CC'). Muscovite mainly exists in the coal matrix and can be partially dissolved by CO₂ (Figure 10 AA'). Organic-clay complexes mainly fill microfractures and are partially dissolved by CO₂ (Figure 10 BB').

After CO₂ treatment, calcite, dolomite, and other carbonate minerals in the coal matrix (including those that fill pores) dissolve or partially dissolve, forming a large number of pores created by dissolution (Figure 11a and 11c). The shape of these dissolution-created pores is irregular, and the pore diameter is generally <10 μm. Residual carbonate minerals can be found in these pores. These dissolution-created pores are the primary cause of the changes in the number and volume of pores <10 μm in diameter, and they control the changes in the pore number distribution in the coal samples (Figure 11a and 11c). Some of the pores created by dissolution become connected to each other (Figure 11a) and with microfractures (Figure 11c); however, most of them are associated with local connectivity in a small part of coal samples, which are characterized by overall poor connectivity. Therefore, these pores make a weak contribution to the connectivity of the coal samples.



Note: a and c are coal samples from the Xinjing Mine; c is a coal sample from the Sihe Mine; d is a coal sample from the Yuwu Mine.

Figure 11—Pores, microfractures, and minerals in coal samples before and after CO₂ treatment.

After CO₂ treatment, the carbonate minerals, such as calcite and dolomite, with grain sizes >50 μm in the coal matrix (including those filling pores) are dissolved or partially dissolved, forming dissolution-created pores with diameters >50 μm (Figure 11b). Residual carbonate minerals can also be found in the pores created by dissolution (Figure 11b). These dissolution-created pores have a relatively large contribution to the number of pores >50 μm in diameter after CO₂ treatment, while they have a relatively small contribution to the pore volume. Similar to the dissolution-created pores <10 μm in diameter, the connectivity of the dissolution-created pores with diameters >50 μm is weak. A large number of carbonate minerals filling the micro-fractures are dissolved by CO₂, resulting in a partial or complete opening of the micro-fractures and significantly increasing the apertures of the micro-fractures (Figure 11c). Although the number of micro-fractures is less than the number of dissolution-created pores >50 μm in diameter caused by CO₂ and has a much smaller contribution to the pore number, the volume of micro-fractures is much larger than that of dissolution-created pores >50 μm in diameter, and micro-fractures are the main contributor to the increase in the volume of pores >50 μm in diameter. This increase is also the reason why the pore volumes of the coal samples increase significantly after CO₂ treatment, while the pore numbers change only slightly. Furthermore, according to Section 3.2.3, the connectivity of coal samples on the micrometer scale is mainly contributed by microfractures. Therefore, increasing the microfracture aperture significantly improves the connectivity of the coal samples and throat lengths. Moreover, some micro-fractures are filled with organic-clay complexes. After CO₂ treatment, several organic-clay complexes that fill the microfractures are removed, which also increase the apertures and connectivity of the microfractures. In general, microfractures in coal samples are mainly filled with carbonate minerals (Figure 10), and the removal of organic-clay complexes from microfractures has a

relatively weak effect on microfractures. Furthermore, neither the clay minerals in the coal matrix nor the clay minerals that fill the microfractures exhibit obvious changes after CO₂ treatment, and their influence on the structure of the pore fracture and the connectivity of the coal is weak (**Figure 11d**).

Conclusions

In this paper, taking low-volatile bituminous coals and anthracite coals collected from the Qinshui basin as examples, changes in pore fracture structure and connectivity on the micron scale after CO₂ treatments were studied using X-ray micro-CT, FESEM and EDS. The following conclusions can be drawn from this study.

1. After CO₂ treatment, the pore contents and volumes of low-volatile bituminous and anthracite coal increase significantly and the changes in pore numbers are small. The increase in pore volume is mainly caused by pores > 50 μm in diameter, while the change in pore number is related to pores <10 μm in diameter. The connectivity of low-volatile bituminous coal and anthracite coal on the micron-scale is mainly contributed by micro-fractures.
2. After CO₂ treatment, the number of pores with coordination numbers >1 and the number of throats >100 μm in length increase significantly, confirming that CO₂ improves the connectivity of pores and fractures; however, the improvement in pore-fracture connectivity is not enough to improve the connectivity of the coal on the micron-scale.
3. After CO₂ treatment, the changes in pore numbers and volumes are mainly caused by the dissolution of carbonate minerals. Calcite, dolomite and other carbonate minerals in the coal matrix dissolve to form a large number of dissolution-created pores <10 μm in diameter. These dissolution-created pores are the main causes of the increase in the number and volume of pores <10 μm in diameter and determine the changes in pore numbers in coal samples. The carbonate minerals that fill the microfractures are greatly dissolved by CO₂, which increases the apertures and connectivity of the microfractures. These microfractures are the main contributor to the increase in the volume of pores >50 μm in diameter and improve the connectivity of coal on the micrometer scale.

Acknowledgments

This study was supported by the National Key Research and Development Plan (No. 2018YFB0605601), the China National Natural Science Foundation (No. 41972168), and the Jiangsu Key Laboratory of Coal-Based Greenhouse Gas Control and Use (No. 2019A001). We would like to thank engineers from the Shanxi CBM Branch of Huabei Oilfield Company and Lu'an Group and a number of research students from China University of Mining and Technology for their assistance in the coal sampling and some experiments.

Conflicts of Interest

The author(s) declare that they have no conflicting interests.

References

- Anggara, F., Sasaki, K., and Sugai, Y. 2013. Mineral Dissolution/Precipitation During CO₂ Injection into Coal Reservoir: A Laboratory Study. *Energy Procedia* **37**:6722-6729.
- Bertier, P., Swennen, R., Laenen, B., et al. 2006. Experimental Identification of CO₂-water-rock Interactions Caused by Sequestration of CO₂ in Westphalian and Buntsandstein Sandstones of the Campine Basin (NE-Belgium). *Journal of Geochemical Exploration* **89**(1): 10-14.
- Dawson, G.K.W., Golding, S.D., Biddle, D., et al. 2015. Mobilization of Elements from Coal Due to Batch Reactor Experiments with CO₂ and Water at 40 °C and 9.5 MPa. *International Journal of Coal Geology* **140**: 63-70.
- Day, S., Duffy, G., Sakurovs, R., et al. 2008. Effect of Coal Properties on CO₂ Sorption Capacity under Supercritical Conditions. *International Journal of Greenhouse Gas Control* **2**(3): 342-352.

- Du, Y., Sang, S., Wang, W., et al. 2018. Experimental Study of the Reactions of Supercritical CO₂ and Minerals in High-Rank Coal under Formation Conditions. *Energy & Fuels* **32**(2): 1115-1125.
- Fujioka, M., Yamaguchi, S., and Nako, M. 2010. CO₂-ECBM Field Tests in the Ishikari Coal Basin of Japan. *International Journal of Coal Geology* **82**(3): 287-298.
- Faiz, M.M., Saghafi, A., Barclay, S.A., et al. 2007. Evaluating Geological Sequestration of CO₂ in Bituminous Coals: The Southern Sydney Basin, Australia as A Natural Analogue. *International Journal of Greenhouse Gas Control* **1**(2): 223-235.
- Hayashi, J., Takeuchi, K., Kusakabe, K., et al. 1991. Removal of Calcium From Low Rank Coals by Treatment with CO₂ Dissolved in Water. *Fuel* **70**(10): 1181-1186.
- Hol, S., Gensterblum, Y., and Massarotto, P. 2014. Sorption and Changes in Bulk Modulus of Coal -Experimental Evidence and Governing Mechanisms for CBM and ECBM Applications. *International Journal of Coal Geology* **128**(12):119-133.
- Kutchko, B.G., Goodman, A.L., Rosenbaum, E., et al. 2013. Characterization of Coal Before and After Supercritical CO₂ Exposure Via Feature Relocation Using Field-Emission Scanning Electron Microscopy. *Fuel* **107**(2): 777-78.
- Kolak, J.J. and Burruss, R.C. 2014. The Use of Solvent Extractions and Solubility Theory to Discern Hydrocarbon Associations in Coal, with Application to The Coal-Supercritical CO₂ System. *Organic Geochemistry* **73**(2): 56-69.
- Liu, S.Q., Ma, J.S., Sang, S.X., et al. 2018. The Effects of Supercritical CO₂ on Mesopore and Macropore Structure in Bituminous and Anthracite Coal. *Fuel* **223**: 32-43.
- Liu, C.J., Wang, G.X., Sang, S.X., et al. 2015. Fractal Analysis in Pore Structure of Coal Under Conditions of CO₂ Sequestration Process. *Fuel* **139**: 125-132.
- Liu, C.J., Wang, G.X., Sang, S.X., et al. 2010. Changes in Pore Structure of Anthracite Coal Associated with CO₂ Sequestration Process. *Fuel* **89**: 2665-2672.
- Liu, S.Q., Sang, S.X., Ma, J.S., et al. 2019. Effects of Supercritical CO₂ on Micropores in Bituminous and Anthracite Coal. *Fuel* **242**: 96-108.
- Liu, S.Q., Sang, S.X., Liu, H. , et al. 2015. Growth Characteristics and Genetic Types of Pores and Fractures in A High-Rank Coal Reservoir of The Southern Qinshui Basin. *Ore Geology Reviews* **64**: 140-151.
- Liu, S.Q., Sang, S.X., Pan, Z.J., et al. 2016. Study of Characteristics and Formation Stages of Macroscopic Natural Fractures in Coal Seam #3 for CBM Development in The East Qinnan Block, Southern Qinshui Basin, China. *Journal of Natural Gas Science and Engineering* **34**(2):1321-1332.
- Liu, S.Q., Sang, S.X., Wang, G.X., et al. 2017. FIB-SEM and X-ray CT Characterization of Interconnected Pores in High-Rank Coal Formed from Regional Metamorphism. *Journal of Petroleum Science and Engineering* **148**(1): 21-32.
- Massarotto, P., Golding, S.D., Bae, J.S., et al. 2010. Changes in Reservoir Properties from Injection of Supercritical CO₂ into Coal Seams-A Laboratory Study. *International Journal of Coal Geology* **82**(34):269-279.
- Pan, Z., Ye, J., Zhou, F., et al. 2018. CO₂ Storage in Coal to Enhance Coalbed Methane Recovery: A Review of Field Experiments in China. *International Geology Review* **60**(5):754-776.
- Perera, M.S. A., Ranjith, P.G., Choi, S.K., et al. 2011. The Effects of Sub-Critical and Super-Critical Carbon Dioxide Adsorption-Induced Coal Matrix Swelling on the Permeability of Naturally Fractured Black Coal. *Energy* **36**(11): 6442-6450.
- Ranjith, P.G. and Perera, M.S A. 2012. Effects of Cleat Performance on Strength Reduction of Coal in CO₂ Sequestration. *Energy* **45**(1):1069-1075.
- Song, W., Yao, J., Ma, J., et al. 2018. Pore-Scale Numerical Investigation into The Impacts of The Spatial and Pore-Size Distributions of Organic Matter on Shale Gas Flow and Their Implications on Multiscale Characterization. *Fuel* **216**:707-721.
- Wang, A., Wei, Y., Yuan, Y., et al. 2017. Coalbed Methane Reservoirs' Pore-Structure Characterization of Different Macrolithotypes in the Southern Junggar Basin of Northwest China. *Marine and Petroleum Geology* **86**: 675-688.
- White, C.M., Smith, D.H., Jones, K.L., et al. 2005. Sequestration of Carbon Dioxide in Coal with Enhanced Coalbed Methane Recovery-A Review. *Energy & Fuels* **19**(3): 659-724.
- Wong, S., Law, D., Deng, X.H., et al. 2007. Enhanced Coalbed Methane and CO₂ Storage in Anthracitic Coals-Micro-Pilot Test at South Qinshui, Shanxi, China. *International Journal of Coal Geology* **1**(2): 215-222.
- Xu, Y., Liu, X., Zhang, P., et al. 2016. Role of Chlorine in Ultrafine Particulate Matter Formation during the Combustion of a Blend of High-Cl Coal and Low-Cl Coal. *Fuel* **184**: 185-191.
- Zerai, B., Saylor, B.Z., and Matisoff, G. 2006. Computer Simulation of CO₂ Trapped Through Mineral Precipitation in the Rose Run Sandstone, Ohio. *Applied Geochemistry* **21**(2): 223-240.

Zhou, H.W., Zhong, J.C., Ren, W.G., et al. 2018. Characterization of Pore-Fracture Networks and Their Evolution at Various Measurement Scales in Coal Samples Using X-Ray MCT and a Fractal Method. *International Journal of Coal Geology* **189**:35-49.

Shiqi Liu is a Professor of geological resources and geological engineering at China University of Mining and Technology, where he has worked as faculty for 9 years. His research interests are in the exploration and development of unconventional gas (coalbed methane, shale gas, coal measure gas), and CO₂ geological storage and utilization. He holds B.S. from the China University Of Petroleum (East China) in information and computer science, M.S. from the China University of Petroleum (East China) in oil and gas field development engineering, and Ph.D. from China University of Mining and Technology in geological resources and geological engineering.

Shuxun Sang is a Professor of geology at China University of Mining and Technology, where he has worked as faculty for 28 years. His research interests are in the exploration and development of unconventional gas (coalbed methane, shale gas, coal measure gas) and in geological storage and utilization of CO₂. He holds a B.S., M.S., and Ph.D. from China University of Mining and Technology, all in geology.

Tian Wang is a doctoral candidate at China University of Mining and Technology. Her research interests are in CO₂ geological storage and utilization. She holds a B.S. from China University of Mining and Technology in geology.

Yi Du is a doctoral candidate at China University of Mining and Technology. Her research interests are in CO₂ geological storage and utilization. She holds a B.S. from China University of Mining and Technology in geology.

Huihuang Fang is a doctoral candidate at China University of Mining and Technology. His research interests are in CO₂ geological storage and utilization. He holds M. S. from China University of Mining and Technology in geological resources and geological engineering.